THE JOURNAL OF PHYSICAL CHEMISTRY Letters

pubs.acs.org/JPCL Letter

Pressure-Dependent Rate Constant Caused by Tunneling Effects: OH + HNO_3 as an Example

Thanh Lam Nguyen and John F. Stanton*

Cite This: J. Phys. Chem. Lett. 2020, 11, 3712−3717 Read Online

ACCESS | Metrics & More | Article Recommendations | Supporting Information

ABSTRACT: Tunneling effects on chemical reactions are well-known and have been unambiguously demonstrated by processes that involve the motion of hydrogen atoms at low temperature. However, the process by which tunneling effects cause a falloff curve (i.e., how reaction rate constants depend on pressure) has apparently not been previously documented. This work points out that falloff curves can indeed be caused by tunneling and explains the effect in simple terms. This is an interesting feature of quantum tunneling, which can appear in low temperature chemistry (such as in atmospheric or interstellar environments). In this Letter, we use high-level coupled-cluster calculations in combination with master-equation methods on the well-studied reaction of OH with HNO_3, which plays an important role in the upper troposphere and lower stratosphere. Our results in combination with available experimental data clearly demonstrate that the tunneling correction depends on not just temperature, but also pressure.

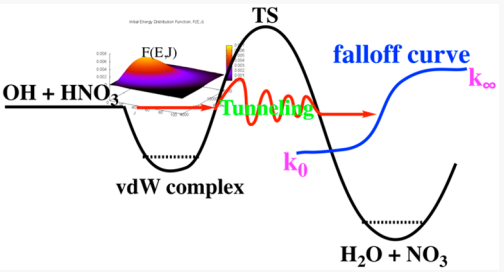

Quantum mechanical tunneling plays a vital role in many fields of chemistry and biology[1] that involve electron transfer processes and/or motions of light atoms such as hydrogen.[2,3] Such light particles can readily pass through a potential barrier even if they do not have sufficient energy to surmount it.[1] Many chemical reactions observed experimentally[4−8] can only be explained by quantum mechanical tunneling effects. Nowadays, the role of tunneling in chemical reactions is fairly well-established.[4−6] This has been seen for several reactions that involve the motion of hydrogen atoms at low temperature (or low energy).[9]

The tunneling correction, $\kappa(T)$,[1,10,11] is defined as the ratio of the quantum mechanical rate coefficient and the (classical mechanical) rate coefficient, the latter of which excludes tunneling effects:

$$\kappa(T) = \frac{k(T)_q}{k(T)_c} = \frac{\int_0^\infty P(E)_q e^{-E/RT} dE}{\int_0^\infty P(E)_c e^{-E/RT} dE} = \frac{\int_0^\infty P(E)_q e^{-E/RT} dE}{\int_{V_o}^\infty e^{-E/RT} dE} \quad (1)$$

where $P(E)_q$ and $P(E)_c$ are quantum and classical transition probabilities, respectively. R is the gas constant, V_o is the potential barrier, and T stands for the temperature of the reaction system. E is the internal energy.

The tunneling correction, a theoretical concept, can be estimated theoretically but cannot be measured experimentally; $\kappa(T)$ is used to determine how important tunneling is for the reaction under study. It is well-established that $\kappa(T)$ is exquisitely sensitive to temperature: it decreases sharply when temperature increases and converges to unity at a sufficiently high temperature.[11] Hence, including an accurate tunneling correction in computing k(T) is vital for reactions occurring in interstellar environments, still significant in atmospheric environments, and ultimately becomes unimportant in high-temperature combustion.

According to the Lindemann−Hinshelwood mechanism,[12,13] the rate coefficient for a unimolecular reaction depends not only on temperature but also on pressure, the latter effect causing a falloff curve. Therefore, the tunneling correction (eq 1) would be a function of pressure as well as temperature (i.e., $\kappa(T, P)$). However, to the best of our knowledge, the pressure dependence of κ has not previously been discussed in the literature. In addition to unimolecular reactions, some bimolecular reactions that take place through one (or more) intermediate species before yielding products are also generally seen to be pressure-dependent.[14] The purpose of this work is to examine the largely unexplored pressure dependence of $\kappa(T)$ and to check whether there is a connection between quantum mechanical tunneling and the falloff curve. The reaction of OH and HNO_3, which significantly affects stratospheric ozone, the HO_x budget, as well as NO_x partitioning in the upper troposphere and lower stratosphere (UTLS),[15−22] is chosen as an example because this bimolecular reaction (which also displays a pressure dependence) has been well-characterized experimentally.[15−20]

Received: March 5, 2020
Accepted: April 22, 2020
Published: April 22, 2020

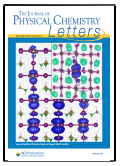

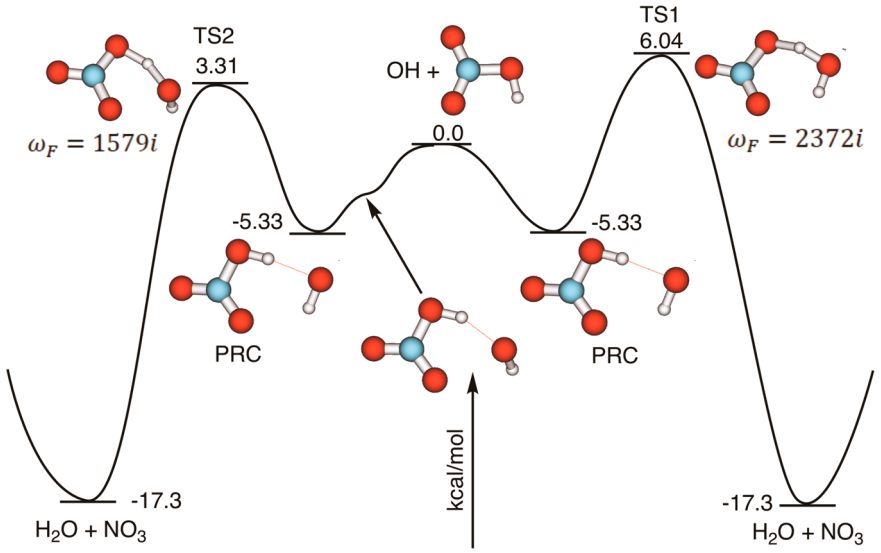

Figure 1. Schematic reaction energy profile for the OH + HNO_3 → H_2O + NO_3 reaction constructed using the mHEAT-345(Q) method.[23] Note that, for the LHS pathway, a shallower van der Waals complex is found with the B3LYP-DFT method,[24,25] but it does not exist at the CCSD(T) level.

The reaction of OH and HNO_3 has been heavily studied but with relatively low levels of theory.[17,24−26] In this work, to obtain high-accuracy energies for kinetics calculations, we used mHEAT-345(Q),[23] which is a composite method mainly based on high-level coupled-cluster calculations including full triple excitations and perturbative noniterative treatment of quadruple excitations. It is reported elsewhere that mHEAT-345(Q) can provide high accuracy for relative energies, typically within 0.5 kcal/mol.[23] The potential energy surface for the OH + HNO_3 reaction is displayed in Figure 1. There are two distinct reaction pathways for the association of OH and HNO_3, depending on the path taken when OH reacts with HNO_3. That on the right-hand-side (RHS) represents the attack of OH in the HNO_3 plane of symmetry, while that on the left-hand-side (LHS) features OH attack roughly perpendicular to the HNO_3 plane of symmetry. The first step of the association is the formation of the van der Waals complex, PRC, which has two hydrogen bonds and a binding energy of 5.33 kcal/mol, which is broadly consistent with an experimental upper limit of 5.3 kcal/mol.[27] It should be mentioned that, for the LHS pathway, a shallower van der Waals complex has been found with the B3LYP-DFT method,[24,25] but it does not persist at the CCSD(T) level. The CCSD(T) optimization directly gives PRC instead. When formed, PRC prefers to dissociate back to the initial reactants via a loose, variational TS. However, a fraction of PRC undergoes an H-abstraction via TS1 or TS2, leading to products H_2O + NO_3. Depending on the temperature under consideration, PRC can tunnel through (and/or surmount) the barrier. At the atmospheric conditions considered in this work, most such product is formed by tunneling through the barrier. As seen in Figure 1, TS1 (with ω_F = 2372i) lies about 3 kcal/mol higher than TS2 (with ω_F = 1579i), but has a notably thinner barrier. So, both reaction pathways are in competition. A theoretical kinetics analysis is desired to quantify product branching ratios and phenomenological rate coefficients.

An *E*,*J*-resolved two-dimensional master equation[28−31] that describes the time evolution of one well (PRC) and multiple products (as shown in Figure 1) is given by

$$\frac{\partial C_1(E_i, J_i, t)}{\partial t} = \sum_{J_k=0}^{J_{max}} \int_{E_k=0}^{E_{max}} \omega_{LJ} P(E_i, J_i | E_k, J_k) C_1(E_k, J_k, t)\, dE_k - \omega_{LJ} C_1(E_i, J_i, t) - \sum_{l=2}^{4} k_{1\to l}(E_i, J_i) C_1(E_i, J_i, t) + \mathrm{OST}(E_i, J_i) \quad (2)$$

where J_{max} is the maximum angular momentum; E_{max} is the maximum internal energy; $C_1(E_i, J_i, t)$ represents the population density of PRC in state (E_i, J_i) and time t; ω_{LJ} (in s^{-1}) is the Lennard−Jones collisional frequency; and $k_{1\to l}(E_i, J_i)$ (in s^{-1}) is the (E_i, J_i)-resolved microcanonical rate coefficient from PRC to products. For the dissociations of PRC via TS1 and TS2, Miller's semiclassical TST (SCTST) theory,[32−36] which includes coupled vibrations and multidimensional tunneling, is used to compute the microcanonical rate constants without angular momentum effects, $k(E,J = 0)$; the J effects are then included using the J-shifting approximation,[3,37,38] assuming an active K-rotor model for both reactant and TS.[39−41] For the barrierless dissociation of PRC back to OH + HNO_3, variational RRKM theory[42,43] is used to characterize a kinetic bottleneck as well as to compute $k(E, J)$ for a loose TS. $P(E_i, J_i \mid E_k, J_k)$ is the *E*,*J*-resolved collisional transfer probability distribution function from state (E_k, J_k) to state (E_i, J_i). OST stands for the original source term, and is given by

$$\mathrm{OST}(E_i, J_i) = F_{PRC}(E_i, J_i) k_\infty(T)[\mathrm{OH}][\mathrm{HNO_3}] \quad (3)$$

where $k_\infty(T)$ is the capture rate constant for the association step of OH and HNO_3, leading to population in the PRC. $F_{PRC}(E_i, J_i)$ is the *E*,*J*-resolved initial distribution function for the nascent energized PRC and given by[44,45]

https://dx.doi.org/10.1021/acs.jpclett.0c00733
J. Phys. Chem. Lett. 2020, 11, 3712−3717

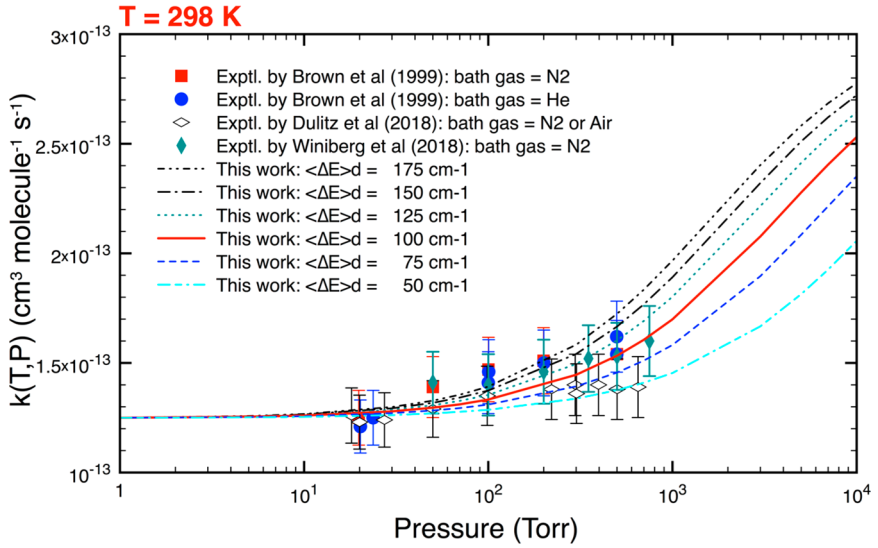

Figure 2. Reaction rate constants calculated at 298 K as functions of pressure and average vibrational and rotational energies transferred in a downward direction. Here, we choose $\langle \Delta E \rangle_d = \langle \Delta E_{vib} \rangle_d = \langle \Delta E_{rot} \rangle_d$ (results for different values of $\langle \Delta E_{vib} \rangle_d$ and $\langle \Delta E_{rot} \rangle_d$ are provided in the Supporting Information). Where possible, experimental data[15−17] are also included for the purpose of comparison. Note that pressure dependence in the calculated rate constants is conspicuous; that for the experimental data is simply suggestive, owing to the limited range of pressure studied.

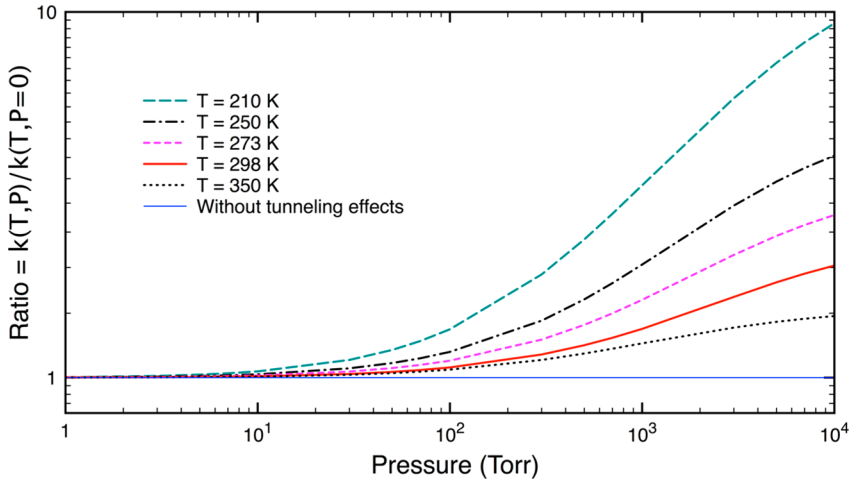

Figure 3. A ratio of $k(T,P)$ and $k(T,P = 0)$ calculated as a function of both temperature and pressure. Note that this ratio is also equivalent to the ratio of tunneling corrections (κ) at P and $P = 0$ (see text).

$$F_{PRC}(E_i, J_i) = \frac{(2J_i + 1)k_{1\rightarrow OH}(E_i, J_i)\rho_1(E_i, J_i)\exp(-E_i/RT)}{\sum_{J_i=0}^{J_{max}}(2J_i + 1)\int_{E_i=0}^{E_{max}} k_{1\rightarrow OH}(E_i, J_i)\rho_1(E_i, J_i)\exp(-E_i/RT)dE_i} \quad (4)$$

In eq 4, $\rho_1(E_i,J_i)$ is the density of rovibrational states for PRC.

The mHEAT calculations mentioned above provide structures, energies, rovibrational parameters, and anharmonic constants for all relevant stationary points. These data are then used as input to the two-dimensional master equation (2DME), which depends on both internal energy and total angular momentum, to obtain thermal rate constants (as well as product yields) as a function of both temperature and pressure. Algorithms for solution of the 2DME were previously reported elsewhere[46−50] and are briefly summarized in the Supporting Information.

Figure 2 displays thermal rate constants calculated at 298 K as a function of pressure (i.e., falloff curves) for the OH + HNO_3 reaction. Three sets of recent experimental data[15−17] are also included for comparison. Because both the average vibrational ($\langle \Delta E_{vib} \rangle_d$) and rotational ($\langle \Delta E_{rot} \rangle_d$) energies transferred in a downward direction by collisions between the vibrationally excited PRC and the bath gas are unknown, a trial and error process is used to determine them. $\langle \Delta E \rangle_d$ is varied from 50 to 175 cm^{-1} with a step size of 25 cm^{-1}. As seen in Figure 2, all calculated $k(T,P)$ are in good agreement (within 20%) with the experimental results.[15−17] Theory with $\langle \Delta E \rangle_d = 50$ cm^{-1} agrees with the experiment of Dulitz et al.,[16] while a higher value of $\langle \Delta E \rangle_d = 175$ cm^{-1} is desirable to match the experimental results of Brown et al.[15] The overall best fit between theory and experiment in this scenario is found with $\langle \Delta E \rangle_d \sim 100$ cm^{-1}. Following the same strategy, we did the same at other temperatures (from 210 to 350 K), where experimental data are available,[15−17] and a good agreement

https://dx.doi.org/10.1021/acs.jpclett.0c00733
J. Phys. Chem. Lett. 2020, 11, 3712−3717

between theory and experiment has been seen (see Figure S1 in the Supporting Information).

It should be emphasized that other approaches for kinetics calculations could be used to generate the same qualitative results. For example, there are several master-equation approaches from other groups (refs 28−31), which can be used in a manner similar to that above. In addition, the PolyRate software package (ref 11) can be used to compute thermal rate constants at the high-pressure limit, where Boltzmann thermal equilibrium distribution can be assumed. Our recent studies for several reactions have shown that the SCTST approach is comparable in accuracy to other methods used for tunneling, as for example those used in PolyRate. It might also be mentioned that a classical trajectory approach would not reproduce the falloff curve here because tunneling effects are not included. Full quantum dynamics are also not practical, both because they are not suited to capture pressure effects as well as the very high dimensionality of the reactive potential energy surface.

Is κ a function of pressure? Next, we calculated the ratio of $k(T,P)$ to $k(T,P = 0)$ as a function of both pressure and temperature and plotted the results in Figure 3. As demonstrated in the Supporting Information, this ratio (γ) is also equivalent to the ratio of $\kappa(T,P)$ and $\kappa(T,P = 0)$. Note that when tunneling is turned off, the rate constant without the tunneling correction, $k(T)_{wt}$, becomes pressure-independent in this scenario, as seen below.

$$\gamma = \frac{k(T,P)}{k(T,P=0)} = \frac{\kappa(T,P)\times k(T,P)_{wt}}{\kappa(T,P=0)\times k(T,P=0)_{wt}} = \frac{\kappa(T,P)}{\kappa(T,P=0)} \quad (5)$$

Figure 3 clearly shows that the tunneling correction (κ) depends not only on temperature, but also on pressure. To the best of our knowledge, this property has not previously been pointed at in the literature. The ratio $\gamma = \kappa(T,P)/\kappa(T,0)$ increases with increasing pressure. In contrast, it decreases with temperature, as is expected. From Figure 3, it is obvious that γ is most conspicuous at low temperature, and reduces significantly when temperature increases. γ can be used to determine whether or not a reaction depends on pressure as well as the shape of the falloff curve. At conditions of 298 K and 760 Torr, the calculated value of γ is 1.30, meaning that the rate constant is only 30% larger than at the zero-pressure limit. Such a small difference may not easily be observed in experiment for two reasons: first, many experiments have been done in the low-pressure regime (≪760 Torr) where the pressure dependence is smaller (see Figure 3); second, experimental values tend to have an error bar of about 10 to 20%. To observe this pressure dependence, experiments would have to be carried out at lower temperatures and/or higher pressures.

Is there a correlation between tunneling and falloff curve? Scheme 1 reveals a (simplified) kinetics model to compute reaction rate constants at the zero- and infinite-pressure limits.

At the zero-pressure limit, $k(T)_{P=0}$ is calculated as an integral of $G^{\ddagger}_{rv}(E,J)$, which is a sum of rovibrational states including quantum mechanical tunneling correction, from the energy level of the initial reactants, OH + HNO_3, to infinity (because there are no collisions to cause deactivation).

Scheme 1. Schematic Chemical Kinetics Model for the OH + HNO_3 → H_2O + NO_3 Reaction

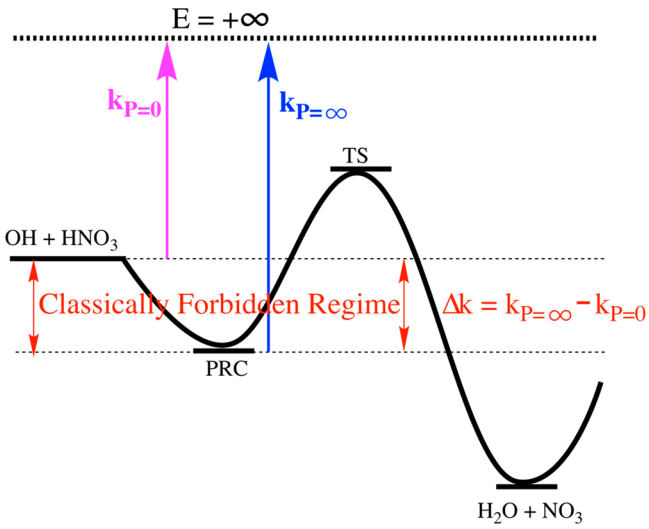

$$k(T)_{P=0} = \frac{1}{h}\times\frac{Q_e^{\ddagger}Q_t^{\ddagger}}{Q_{OH}Q_{HNO_3}}\times\sum_{J=0}^{\infty}\int_0^{\infty}(2J+1)G^{\ddagger}_{rv}(E,J)\exp\left(-\frac{E}{RT}\right)dE \quad (6)$$

At the high-pressure limit, $k(T)_{P=\infty}$ is calculated as an integral of $G^{\ddagger}_{rv}(E,J)$ from the ground energy level of PRC to infinity:

$$k(T)_{P=\infty} = \frac{1}{h}\times\frac{Q_e^{\ddagger}Q_t^{\ddagger}}{Q_{OH}Q_{HNO_3}}\times\sum_{J=0}^{\infty}\int_{-E_{PRC}}^{\infty}(2J+1)G^{\ddagger}_{rv}(E,J)\exp\left(-\frac{E}{RT}\right)dE \quad (7)$$

From eq 7 and eq 6, the difference (Δk) of two rate constants calculated at the infinite- and zero-pressure limits can be derived:

$$\Delta k = k(T)_{P=\infty} - k(T)_{P=0} = \frac{1}{h}\times\frac{Q_e^{\ddagger}Q_t^{\ddagger}}{Q_{OH}Q_{HNO_3}}\times\sum_{J=0}^{\infty}\int_{-E_{PRC}}^{0}(2J+1)G^{\ddagger}_{rv}(E,J)\exp\left(-\frac{E}{RT}\right)dE \quad (8)$$

Δk in eq 8 comprises an integral of $G^{\ddagger}_{rv}(E,J)$ calculated from the lowest energy level of the PRC to that of OH + HNO_3, a region that lies in a classically forbidden regime (see Scheme 1). When tunneling is turned off, Δk becomes zero, resulting in $k(T)_{P=\infty} = k(T)_{P=0}$. In order words, the reaction is pressure-independent in the absence of tunneling. Thus, we can conclude that tunneling effects make this reaction depend on pressure (i.e., producing a falloff curve), which is an interesting perspective and observation. Notably, this finding is consistent with experimental results for OH + HNO_3 (which has a pressure dependence because tunneling effects are important)[15−17] and those for OD + DNO_3 (which is pressure-independent because tunneling effects are unimportant).[51] It is also important to point out that the magnitude of Δk implies the degree to which the reaction depends on pressure, as well as the shape of the falloff curve. The magnitude of Δk can be

https://dx.doi.org/10.1021/acs.jpclett.0c00733
J. Phys. Chem. Lett. 2020, 11, 3712−3717

influenced by a number of factors, including a strongly bound PRC, the barrier height (energy of the TS), and the shape of the barrier. All three factors control quantum mechanical transition probabilities through the barrier leading to products, $H_2O + NO_3$.

While a tunneling enhancement of the rate constant at the high-pressure limit might well be similarly demonstrated with the simple Lindemann model, the master-equation approach used here is more general and provides a means to compute the experimental falloff curve, and to investigate the tunneling effects therein.

In summary, high accuracy coupled-cluster calculations in combination with a fully *E,J*-resolved two-dimensional master equation simulation[52] have been used to study the reaction of OH and HNO_3 to produce $H_2O + NO_3$. The calculated results, in combination with the available experimental data, clearly show that the tunneling correction, $\kappa(T,P)$, is a function of both temperature and pressure. Moreover, tunneling effects are found to be the source of the pressure dependence. This interesting feature of quantum mechanical tunneling, which has a relatively simple origin, is elucidated and explained in terms of an elementary construction. Given that reactions similar to OH + HNO_3 with H-abstraction following formation of a van der Waals complex are very common in atmosphere and interstellar chemistry,[22,53,54] the results of this work may be applicable to such environments.

■ ASSOCIATED CONTENT

Supporting Information

The Supporting Information is available free of charge at https://pubs.acs.org/doi/10.1021/acs.jpclett.0c00733.

Theoretical methods, optimized geometries, and rovibrational parameters for various stationary points as well as additional results are provided (PDF)

■ AUTHOR INFORMATION

Corresponding Author

John F. Stanton − *Quantum Theory Project, Department of Chemistry and Physics, University of Florida, Gainesville, Florida 32611, United States;* orcid.org/0000-0003-2345-9781; Email: johnstanton@ufl.edu

Author

Thanh Lam Nguyen − *Quantum Theory Project, Department of Chemistry and Physics, University of Florida, Gainesville, Florida 32611, United States;* orcid.org/0000-0002-7794-9439

Complete contact information is available at: https://pubs.acs.org/10.1021/acs.jpclett.0c00733

Notes

The authors declare no competing financial interest.

■ ACKNOWLEDGMENTS

Work at the University of Florida was supported by the U.S. National Science Foundation (Grant CHE-1664325) and Department of Energy, Office of Science, Office of Basic Energy Sciences under Award DE-FG02-07ER15884.

■ REFERENCES

(1) Bell, R. P. *The tunnel effect in chemistry*; Chapman and Hall: London, New York, 1980; p 222.

(2) Truhlar, D. G.; Garrett, B. C.; Klippenstein, S. J. Current status of transition-state theory. *J. Phys. Chem.* **1996**, *100* (31), 12771−12800.

(3) Miller, W. H. Tunneling Corrections to Unimolecular Rate Constants, with Application to Formaldehyde. *J. Am. Chem. Soc.* **1979**, *101* (23), 6810−6814.

(4) Schreiner, P. R.; Reisenauer, H. P.; Ley, D.; Gerbig, D.; Wu, C. H.; Allen, W. D. Methylhydroxycarbene: Tunneling Control of a Chemical Reaction. *Science* **2011**, *332* (6035), 1300−1303.

(5) Schreiner, P. R. Tunneling Control of Chemical Reactions: The Third Reactivity Paradigm (vol 139, pg 15276, 2017). *J. Am. Chem. Soc.* **2018**, *140* (4), 1566−1566.

(6) Shannon, R. J.; Blitz, M. A.; Goddard, A.; Heard, D. E. Accelerated chemistry in the reaction between the hydroxyl radical and methanol at interstellar temperatures facilitated by tunnelling. *Nat. Chem.* **2013**, *5* (9), 745−749.

(7) Martin, J. C. G.; Caravan, R. L.; Blitz, M. A.; Heard, D. E.; Plane, J. M. C. Low Temperature Kinetics of the CH3OH + OH Reaction. *J. Phys. Chem. A* **2014**, *118* (15), 2693−2701.

(8) Acharyya, K.; Herbst, E.; Caravan, R. L.; Shannon, R. J.; Blitz, M. A.; Heard, D. E. The importance of OH radical-neutral low temperature tunnelling reactions in interstellar clouds using a new model. *Mol. Phys.* **2015**, *113* (15−16), 2243−2254.

(9) Nguyen, T. L.; Xue, B. C.; Weston, R. E.; Barker, J. R.; Stanton, J. F. Reaction of HO with CO: Tunneling Is Indeed Important. *J. Phys. Chem. Lett.* **2012**, *3* (11), 1549−1553.

(10) Truhlar, D. G.; Hase, W. L.; Hynes, J. T. Current Status of Transition-State Theory. *J. Phys. Chem.* **1983**, *87* (15), 2664−2682.

(11) Truhlar, D. G.; et al. *POLYRATE 2015*: Computer Program for the Calculation of Chemical Reaction Rates for Polyatomics; 2015.

(12) Laidler, K. J. Chemical-Kinetics and the Origins of Physical-Chemistry. *Arch Hist Exact Sci.* **1985**, *32* (1), 43−75.

(13) King, M. C.; Laidler, K. J. Chemical-Kinetics and the Radiation Hypothesis. *Arch Hist Exact Sci.* **1984**, *30* (1), 45−86.

(14) Weston, R. E.; Nguyen, T. L.; Stanton, J. F.; Barker, J. R. HO +CO Reaction Rates and H/D Kinetic Isotope Effects: Master Equation Models with ab Initio SCTST Rate Constants. *J. Phys. Chem. A* **2013**, *117* (5), 821−835.

(15) Brown, S. S.; Talukdar, R. K.; Ravishankara, A. R. Reconsideration of the rate constant for the reaction of hydroxyl radicals with nitric acid. *J. Phys. Chem. A* **1999**, *103* (16), 3031−3037.

(16) Dulitz, K.; Amedro, D.; Dillon, T. J.; Pozzer, A.; Crowley, J. N. Temperature-(208−318 K) and pressure-(18−696 Torr) dependent rate coefficients for the reaction between OH and HNO3. *Atmos. Chem. Phys.* **2018**, *18* (4), 2381−2394.

(17) Winiberg, F. A. F.; Percival, C. J.; Shannon, R.; Khan, M. A. H.; Shallcross, D. E.; Liu, Y. D.; Sander, S. P. Reaction kinetics of OH + HNO3 under conditions relevant to the upper troposphere/lower stratosphere. *Phys. Chem. Chem. Phys.* **2018**, *20* (38), 24652−24664.

(18) Atkinson, R. Gas-Phase Tropospheric Chemistry of Volatile Organic Compounds: 1. Alkanes and Alkenes. *J. Phys. Chem. Ref. Data* **1997**, *26*, 215−290.

(19) Stachnik, R. A.; Molina, L. T.; Molina, M. J. Pressure and Temperature Dependences of the Reaction of Oh with Nitric-Acid. *J. Phys. Chem.* **1986**, *90* (12), 2777−2780.

(20) Margitan, J. J.; Watson, R. T. Kinetics of the Reaction of Hydroxyl Radicals with Nitric-Acid. *J. Phys. Chem.* **1982**, *86* (19), 3819−3824.

(21) Gille, J. C.; Russell, J. M.; Bailey, P. L.; Remsberg, E. E.; Gordley, L. L.; Evans, W. F. J.; Fischer, H.; Gandrud, B. W.; Girard, A.; Harries, J. E.; Beck, S. A. Accuracy and Precision of the Nitric-Acid Concentrations Determined by the Limb Infrared Monitor of the Stratosphere Experiment on Nimbus-7. *J. Geophys Res-Atmos* **1984**, *89* (Nd4), 5179−5190.

(22) Smith, I. W. M. Laboratory studies of atmospheric reactions at low temperatures. *Chem. Rev.* **2003**, *103* (12), 4549−4564.

(23) Thorpe, J. H.; Lopez, C. A.; Nguyen, T. L.; Baraban, J. H.; Bross, D. H.; Ruscic, B.; Stanton, J. F. High-accuracy extrapolated ab

initio thermochemistry. IV. A modified recipe for computational efficiency. *J. Chem. Phys.* **2019**, *150* (22), 224102.
(24) Xia, W. S.; Lin, M. C. A multifacet mechanism for the OH +HNO3 reaction: An ab initio molecular orbital/statistical theory study. *J. Chem. Phys.* **2001**, *114* (10), 4522−4532.
(25) Gonzalez, J.; Anglada, J. M. Gas Phase Reaction of Nitric Acid with Hydroxyl Radical without and with Water. A Theoretical Investigation. *J. Phys. Chem. A* **2010**, *114* (34), 9151−9162.
(26) Lamb, J. J.; Mozurkewich, M.; Benson, S. W. Negative Activation-Energies and Curved Arrhenius Plots 0.3. Oh + Hno-3 and Oh + Hno-4. *J. Phys. Chem.* **1984**, *88* (25), 6441−6448.
(27) O'Donnell, B. A.; Li, E. X. J.; Lester, M. I.; Francisco, J. S. Spectroscopic identification and stability of the intermediate in the OH+HONO2 reaction. *Proc. Natl. Acad. Sci. U. S. A.* **2008**, *105* (35), 12678−12683.
(28) Jeffery, S. J.; Gates, K. E.; Smith, S. C. Full Iterative Solution of the Two-Dimensional Master Equation for Thermal Unimolecular Reactions. *J. Phys. Chem.* **1996**, *100*, 7090−7096.
(29) Robertson, S. H.; Pilling, M. J.; Green, N. J. B. Diffusion approximations of the two-dimensional master equation. *Mol. Phys.* **1996**, *89* (5), 1531−1551.
(30) Robertson, S. H.; Pilling, M. J.; Gates, K. E.; Smith, S. C. Application of inverse iteration to 2-dimensional master equations. *J. Comput. Chem.* **1997**, *18* (8), 1004−1010.
(31) Jasper, A. W.; Pelzer, K. M.; Miller, J. A.; Kamarchik, E.; Harding, L. B.; Klippenstein, S. J. Predictive a priori pressure-dependent kinetics. *Science* **2014**, *346* (6214), 1212−1215.
(32) Miller, W. H. Semiclassical Theory for Non-Separable Systems - Construction of Good Action-Angle Variables for Reaction-Rate Constants. *Faraday Discuss. Chem. Soc.* **1977**, *62*, 40−46.
(33) Miller, W. H.; Hernandez, R.; Handy, N. C.; Jayatilaka, D.; Willetts, A. Abinitio Calculation of Anharmonic Constants for a Transition-State, with Application to Semiclassical Transition-State Tunneling Probabilities. *Chem. Phys. Lett.* **1990**, *172* (1), 62−68.
(34) Hernandez, R.; Miller, W. H. Semiclassical Transition-State Theory - a New Perspective. *Chem. Phys. Lett.* **1993**, *214* (2), 129−136.
(35) Nguyen, T. L.; Stanton, J. F.; Barker, J. R. A practical implementation of semi-classical transition state theory for polyatomics. *Chem. Phys. Lett.* **2010**, *499* (1−3), 9−15.
(36) Nguyen, T. L.; Stanton, J. F.; Barker, J. R. Ab Initio Reaction Rate Constants Computed Using Semiclassical Transition-State Theory: HO+H-2 -> H2O+H and Isotopologues. *J. Phys. Chem. A* **2011**, *115* (20), 5118−5126.
(37) Zhang, D. H.; Light, J. C.; Lee, S. Y. Quantum rate constants for the H-2+OH reaction with the centrifugal sudden approximation. *J. Chem. Phys.* **1998**, *109* (1), 79−86.
(38) Bowman, J. M. Reduced Dimensionality Theory of Quantum Reactive Scattering. *J. Phys. Chem.* **1991**, *95* (13), 4960−4968.
(39) Aubanel, E. E.; Wardlaw, D. M.; Zhu, L.; Hase, W. L. Role of Angular-Momentum in Statistical Unimolecular Rate Theory. *Int. Rev. Phys. Chem.* **1991**, *10* (3), 249−286.
(40) Zhu, L.; Chen, W.; Hase, W. L.; Kaiser, E. W. Comparison of Models for Treating Angular-Momentum in Rrkm Calculations with Vibrator Transition-States - Pressure and Temperature-Dependence of Cl+C2h2 Association. *J. Phys. Chem.* **1993**, *97* (2), 311−322.
(41) Zhu, L.; Hase, W. L. Comparison of Models for Calculating the Rrkm Unimolecular Rate Constant-K(E,J). *Chem. Phys. Lett.* **1990**, *175* (1−2), 117−124.
(42) Truhlar, D. G.; Garrett, B. C. Variational Transition-State Theory. *Annu. Rev. Phys. Chem.* **1984**, *35*, 159−189.
(43) Hase, W. L. Variational Unimolecular Rate Theory. *Acc. Chem. Res.* **1983**, *16* (7), 258−264.
(44) Holbrook, K. A.; Pilling, M. J.; Robertson, S. H.; Robinson, P. J. *Unimolecular reactions*, 2nd ed.; Wiley: Chichester, New York, 1996; p 417.
(45) Forst, W. *Unimolecular reactions: a concise introduction*; Cambridge University Press: Cambridge, U.K., New York, 2003; p 319.
(46) Nguyen, T. L.; Stanton, J. F. A Steady-State Approximation to the Two-Dimensional Master Equation for Chemical Kinetics Calculations. *J. Phys. Chem. A* **2015**, *119* (28), 7627−7636.
(47) Nguyen, T. L.; Lee, H.; Matthews, D. A.; McCarthy, M. C.; Stanton, J. F. Stabilization of the Simplest Criegee Intermediate from the Reaction between Ozone and Ethylene: A High-Level Quantum Chemical and Kinetic Analysis of Ozonolysis. *J. Phys. Chem. A* **2015**, *119* (22), 5524−5533.
(48) Nguyen, T. L.; McCaslin, L.; McCarthy, M. C.; Stanton, J. F. Communication: Thermal unimolecular decomposition of syn-CH3CHOO: A kinetic study. *J. Chem. Phys.* **2016**, *145* (13), 131102.
(49) Nguyen, T. L.; Thorpe, J. H.; Bross, D. H.; Ruscic, B.; Stanton, J. F. Unimolecular Reaction of Methyl Isocyanide to Acetonitrile: A High-Level Theoretical Study. *J. Phys. Chem. Lett.* **2018**, *9* (10), 2532−2538.
(50) Nguyen, T. L.; Ruscic, B.; Stanton, J. F. A master equation simulation for the (OH)-O-center dot + CH3OH reaction. *J. Chem. Phys.* **2019**, *150* (8), 084105.
(51) Brown, S. S.; Burkholder, J. B.; Talukdar, R. K.; Ravishankara, A. R. Reaction of hydroxyl radical with nitric acid: Insights into its mechanism. *J. Phys. Chem. A* **2001**, *105* (9), 1605−1614.
(52) Nguyen, T. L.; Stanton, J. F. Pragmatic Solution for a Fully *E,J*-Resolved Master Equation. *J. Phys. Chem. A* **2020**, *124*, 2907.
(53) Smith, I. W. M.; Ravishankara, A. R. Role of hydrogen-bonded intermediates in the bimolecular reactions of the hydroxyl radical. *J. Phys. Chem. A* **2002**, *106* (19), 4798−4807.
(54) Troe, J. The Polanyi Lecture - the Colorful World of Complex-Forming Bimolecular Reactions. *J. Chem. Soc., Faraday Trans.* **1994**, *90* (16), 2303−2317.

https://dx.doi.org/10.1021/acs.jpclett.0c00733
J. Phys. Chem. Lett. 2020, 11, 3712−3717